Introduction

These are notes for two lectures on "Neutron Star Theory" at the CRAQ Summer School, held in Montreal in August 2016.

Neutron stars are important for many reasons: they are endpoints of stellar evolution, they contain unique phases of matter that exist only at high pressure, they have strong magnetic fields, strong gravity, the precise timing of pulsars enables tests of general relativity, and hopefully soon as a source of gravitational radiation from mergers. Neutron star theory encompasses far too much to cover in two lectures. I decided here to mostly focus on the interior physics of neutron stars, and how that can be constrained observationally. The notes are divided into three parts: (1) the structure of the neutron star crust and core and the mass-radius relation, (2) neutron star cooling, and (3) a brief discussion of neutron star magnetic field evolution.

Chapter 1

Neutron Star Structure

1.1 Neutron Star Basics

Neutron stars are composed mostly of degenerate neutrons, which provide the pressure required to hold up the star against gravity, just as degenerate electrons hold up a white dwarf. We can get the expected radius of a star held up with neutron degeneracy pressure by scaling from a white dwarf. From hydrostatic balance, the central pressure P_c of a star is roughly given by

$$\frac{P_c}{R} \sim \frac{GM}{R^2}\frac{M}{R^3} \rightarrow P_c \sim \frac{GM^2}{R^4}. \tag{1.1}$$

If the pressure is provided by degenerate particles of mass m,

$$P = \frac{2}{5}nE_F = \frac{2}{5}n\frac{\hbar^2}{2m}(3\pi^2 n)^{2/3}. \tag{1.2}$$

The number density of particles is $n \sim M/R^3$ for both white dwarfs and neutron stars. Therefore

$$P_c \propto \frac{M^{5/3}}{mR^5} \propto \frac{M^2}{R^4} \Rightarrow R \propto M^{-1/3}m^{-1}. \tag{1.3}$$

The radius of the neutron star should be a factor $m_n/m_e \approx 2000$ times smaller than a white dwarf. (An alternative version of this argument is to set $E_F \sim Gm_pM/R$.) For $R_{WD} \approx 10^9$ cm, we get $R_{NS} \approx 5$ km. Not bad – we think that neutron stars are between about 10 and 15 km in radius.

A composition of neutrons may seem surprising if you consider that free neutrons decay with a half-life of about 15 minutes by the reaction

$$n \rightarrow p + e^- + \bar{\nu}_e. \tag{1.4}$$

Yet neutrons are able to exist stably in an atomic nucleus or in a neutron star. The reason is that the reaction (1.4) is in equilibrium with the reverse reaction, electron capture on protons

$$p + e^- \rightarrow n + \nu_e. \tag{1.5}$$

The condition for equilibrium is that the chemical potentials balance

$$\mu_n = \mu_e + \mu_p. \tag{1.6}$$

This is known as beta-equilibrium.

At high density, the equilibrium favors neutrons, which is why we end up with neutron stars. To see this, we write down the chemical potentials for degenerate electrons, neutrons, and protons. All three species of particle are degenerate because their Fermi energies are much greater than any thermal energy ($E_F \gg k_B T$) — neutron stars are *cold stars*. (The energy scale is given by the virial theorem: the energy per baryon must be $\sim GMm_p/R \sim 100$ MeV, which is $\gg k_B T$ as long as $T \ll 10^{12}$ K.) The chemical potentials are then $\mu_n = m_n c^2 + p_{F,n}^2/2m_n$, $\mu_p = m_p c^2 + p_{F,p}^2/2m_p$, and $\mu_e = p_{F,e} c$ (the electrons are relativistic at Fermi energies of ~ 100 MeV). We can neglect the neutron–proton mass difference (~ 1 MeV) compared to the Fermi energies and write $m_n \approx m_p \approx m_u$. Beta-equilibrium implies

$$\frac{p_{F,n}^2}{2m_u} = \frac{p_{F,p}^2}{2m_u} + p_{F,e} c. \tag{1.7}$$

From charge neutrality, $n_e = n_p$, which implies that the electron and proton momenta must be equal $p_{F,e} = p_{F,p}$, where we use the relation $p = \hbar(3\pi^2 n)^{1/3}$ for degenerate particles. This means that the electron term must dominate on the right hand side. This gives the proton to neutron ratio as

$$\frac{n_p}{n_n} \approx \left(\frac{E_{F,n}}{2m_u c^2}\right)^{3/2} \sim \left(\frac{100\ \text{MeV}}{1\ \text{GeV}}\right)^{3/2}, \tag{1.8}$$

or a proton fraction of a few percent.

The picture of a neutron star as a self-gravitating ball of non-interacting fermions is of course simplified. A more realistic slice showing what we think a neutron star looks like is shown in Figure 1.1, which is taken from [17]. The simple model of a n, p, e^- neutron star fails in a few different ways. First, the equation of state of the neutrons and protons in the core is far from being that of an ideal degenerate gas. Instead of $P \propto \rho^{5/3}$, the equation of state is closer to $P \propto \rho^2$ because of interactions between the neutrons and protons. The high Fermi energies also allow the production of other particles such as muons (the mass of the muon is 105.7 MeV), perhaps pions (mass of pion is ≈ 140 MeV), or even quark matter. We discuss this further in section 1.3. Second, we have ignored the temperature of the core which matters for example if we want to know how hot the surface will be and whether we can observe the star. We discuss the cooling of neutron stars in section 2. Finally, near the surface of the star where the density and Fermi energies drop, neutrons and protons prefer to concentrate in bound nuclei rather than exist as homogeneous nuclear matter. The region in which nuclei are present makes up the outer ≈ 1 km of the star known as the crust. We discuss the structure of this interesting region in the next section.

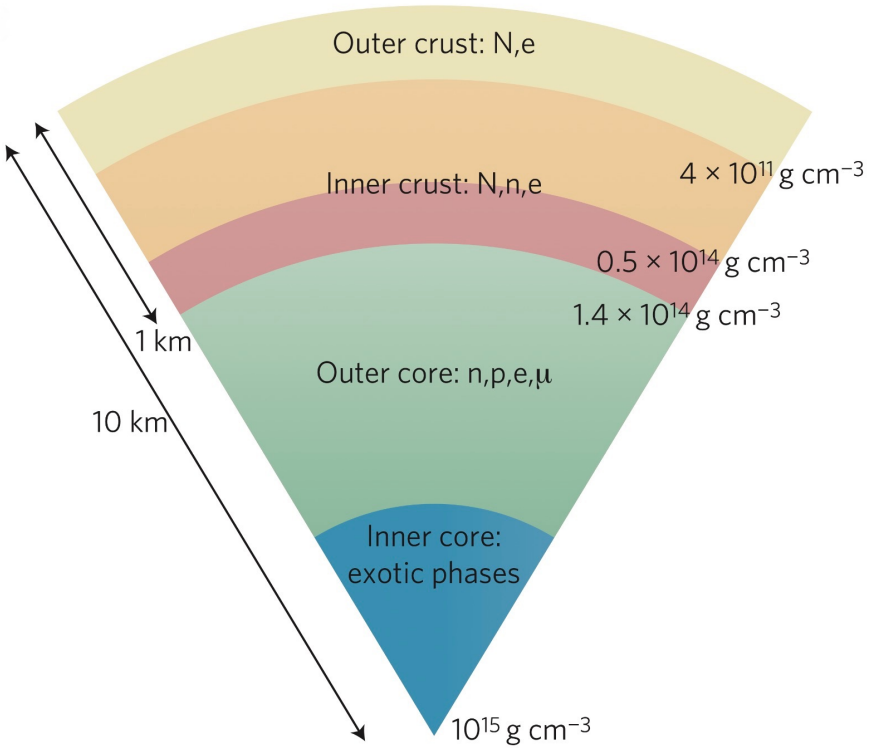

Figure 1.1: The neutron star pizza-diagram showing the different regions of the crust and core. Taken from [17].

1.2 The Neutron Star Crust

1.2.1 What happens to matter as it is compressed

The gas at the surface of a neutron star has about the same density as water, $\rho \sim 1$ g cm^{-3}, but in the core the density is 10^{14}–10^{15} g cm^{-3}. The state of matter is very different in each of these circumstances: ideal gas at the surface, nuclear matter at the centre. How this transformation occurs sets the internal structure of the star: the outermost atmosphere and underlying envelope, the outer crust with its solid lattice of nuclei and degenerate electrons, the inner crust with free neutrons permeating the solid, and the core, with neutrons and protons, and possibly other particles, making up bulk nuclear matter. I start by highlighting the important pieces of physics that determine the transition.

Hydrostatic balance. As you move radially into the star from the surface, the pressure increases to support the increasing weight of the material above any given point. This is hydrostatic balance, $P \approx gy$ where P is the pressure, $g \approx GM/R^2$ is the surface gravity, and y is the mass per unit area or column depth. The scale height is $H = y/\rho = P/\rho g$ (the lengthscale on which pressure changes).

Pressure ionization. The first thing that happens as atoms get pushed together is that

the electrons in one atom begin to feel the electric fields from other atoms. Eventually, the electrons are no longer bound to a single nucleus; the matter is *pressure ionized*. To estimate when this happens, we can ask when is the spacing between atoms roughly equal to the atomic radius $a_Z = a_0/Z$ where $a_0 = \hbar/(\alpha m_e c) = 0.53$Å is the Bohr radius. The spacing between atoms is given by $(4\pi/3)a^3 n = 1$ where the number density is $n = \rho/Am_p$. This gives $a = a_Z$ when

$$\rho = \frac{3Am_p}{4\pi}\left(\frac{\alpha m_e c Z}{\hbar}\right)^3 = 2.7 \text{ g cm}^{-3}\, AZ^3. \tag{1.9}$$

This formula overestimates the density at which pressure ionization occurs; a detailed treatment is given by [6]. The density at the photosphere of the neutron star is ~ 1 g cm^{-3} so for light elements like hydrogen and helium the matter is pressure ionized; heavier elements such as ^{56}Fe are ionized by $\rho \sim 10^4$ g cm^{-3}.

Degenerate electrons. Not too far into the star, then, the atoms are fully ionized and the electrons are free. They form a Fermi gas with Fermi momentum $p_F = \hbar k_F$ where $k_F = (3\pi^2 n_e)^{1/3}$. The Fermi energy is

$$E_F = \frac{p_F^2}{2m_e} \approx 30 \text{ eV}\, \left(\frac{\rho Y_e}{1 \text{ g cm}^{-3}}\right)^{2/3}, \tag{1.10}$$

where the electron fraction Y_e is defined by $\rho Y_e = n_e m_p$ (for a single species $Y_e = Z/A \approx 0.5$). Setting $E_F = k_B T$, we see that the electrons become degenerate at a density

$$\rho Y_e = 6.1 \text{ g cm}^{-3}\, \left(\frac{T}{10^6 \text{ K}}\right)^{3/2}. \tag{1.11}$$

Again, except at the very surface, we expect neutron stars to have degenerate electrons. As density increases, the electron Fermi energy increases and eventually $E_F = m_e c^2$ and the electrons become relativistic. This happens at a density

$$\rho Y_e \approx 3 \times 10^6 \text{ g cm}^{-3}. \tag{1.12}$$

Once the electrons are relativistic, the Fermi energy is

$$E_F \approx p_F c \approx 1 \text{ MeV}\, \left(\frac{\rho Y_e}{10^7 \text{ g cm}^{-3}}\right)^{1/3}. \tag{1.13}$$

The pressure is $P_e = (1/4) n_e E_F = 3 \times 10^{24}$ erg cm^{-3} $(\rho Y_e/10^7 \text{ g cm}^{-3})^{4/3}$, or scale height $H = 3000$ cm $(\rho/10^7 \text{ g cm}^{-3})^{1/3} Y_e^{4/3}/g_{14}$ where $g_{14} = g/10^{14}$ cm s^{-2}.

Solid, liquid, or gas?. The electrons are degenerate, but what about the ions? The ions are non-degenerate with energy set by the thermal energy $\sim k_B T$. As the matter is compressed, the ions get closer together and their Couloumb interaction can become important. This is measured by the ratio $\Gamma = Z^2 e^2/a_i k_B T$, where a_i is the interion spacing. For $\Gamma < 1$, the Coulomb energy between ions is small and the ions behave like a gas. For $\Gamma > 1$ Coulomb interactions begin to dominate the thermal energy. The

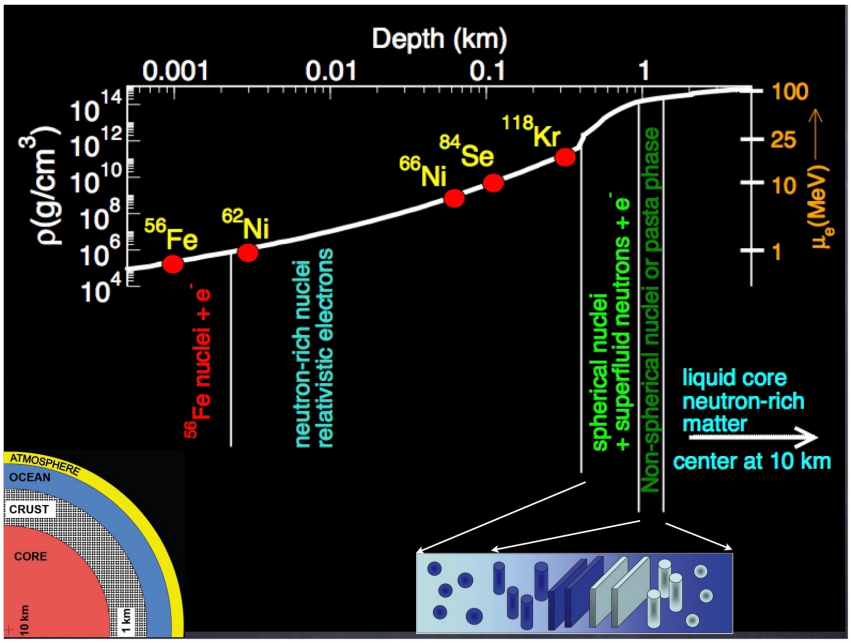

Figure 1.2: The types of nuclei that can be found at different depths in the neutron star crust. The different scales show the depth, the density, and the electron Fermi energy. Taken from [19].

ions behave like a liquid – they know about each other. For $\Gamma \gtrsim 175$, the Coulomb energy is strong enough to force the ions to fall into a lattice, giving a *Coulomb solid*. The neutron star has a solid crust. The density where the ions solidify (where $\Gamma = 175$) is

$$\rho_{\rm solid} \approx 100 \text{ g cm}^{-3} \left(\frac{T}{10^6 \text{ K}}\right)^3 \left(\frac{Z}{26}\right)^{-6} \left(\frac{A}{56}\right). \tag{1.14}$$

Electron captures. Nuclear physics begins to intervene once the electron Fermi energy gets to values of a few MeV and beyond. The nucleus with the largest binding energy (most stable nucleus) is ^{56}Fe. If you let a bunch of neutrons and protons rearrange themselves into whatever nuclei they want, they will form ^{56}Fe to minimize their energy. However, this changes at high density. For $E_F > 3.7$ MeV or $\rho \gtrsim 10^9$ g cm^{-3}, the electron capture reaction

$$^{56}\text{Fe} + e^- \rightarrow ^{56}\text{Mn} \tag{1.15}$$

becomes energetically favourable and so ^{56}Fe is no longer the preferred nucleus (and in fact, note that because even numbers of protons and neutrons are preferred in nuclei, another electron capture reaction would quickly follow to make ^{56}Cr).

The ground state, or lowest energy, nucleus is different at high density. As the electron Fermi energy increases, the ground state nucleus becomes more and more neutron rich (Y_e drops). The high electron Fermi energy outside the nucleus stabilizes the large number of neutrons inside the nucleus that would quickly undergo beta

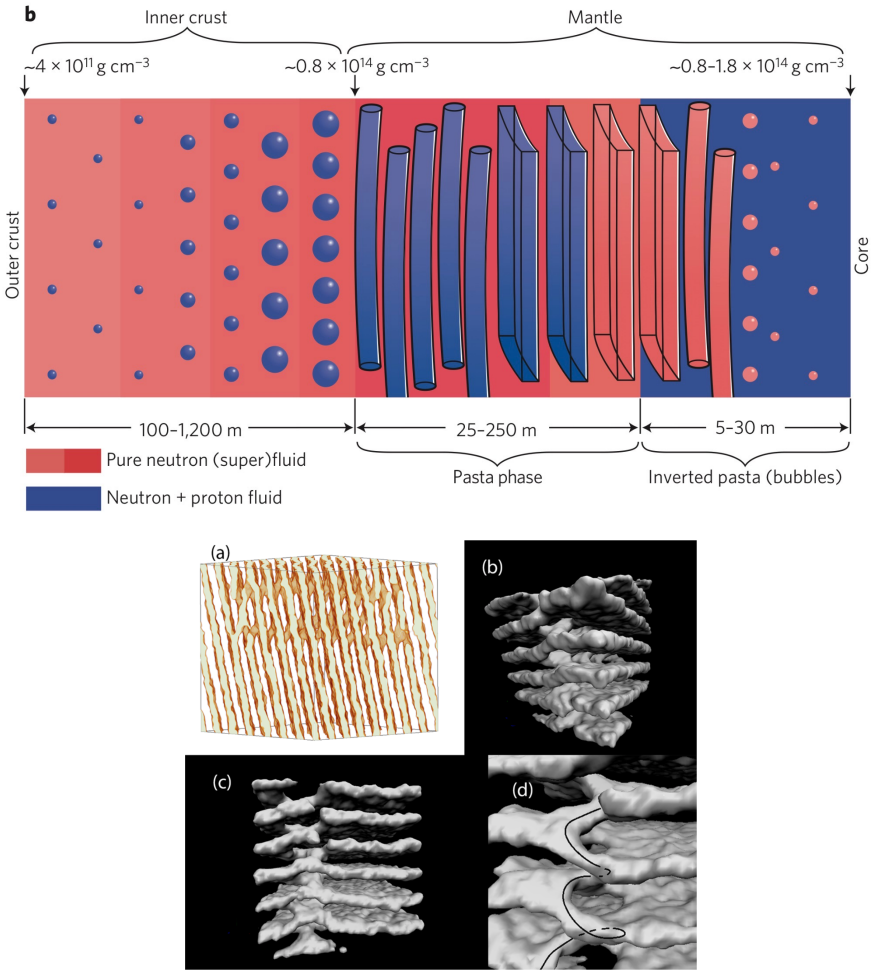

Figure 1.3: Nuclear pasta. Top: An illustration of the transition from normal nuclei through the pasta phases to the core. Taken from [17]. *Bottom:* Lasagna formed in a molecular dynamics simulation. Spiral defects link the lasagna sheets. From [14].

decay in vacuum.

Neutron drip. As density increases, the nuclei become more and more neutron rich. But there is maximum neutron to proton ratio that a nucleus can accommodate. As you try to put more and more neutrons into the nucleus, eventually the nucleus will become unbound. The lowest energy state is then to have free neutrons outside the nucleus. This is known as *neutron drip*. Neutron drip typically occurs for $E_F \approx 27$ MeV or $\rho_{nd} \approx 4 \times 10^{11}$ g cm^{-3}. This point divides the outer crust from the inner crust. Whereas electrons dominate the pressure in the outer crust, the free neutrons set the pressure in the inner crust. Treating them as an ideal Fermi gas, the neutron Fermi energy is $E_{F,n} \approx 1.5$ MeV $\rho_{12}^{2/3} Y_n^{2/3}$ and pressure $P_n = (2/5) n_n E_{F,n} = 5.7 \times 10^{29}$ erg cm^{-3} $(\rho_{12} Y_n)^{5/3}$. The pressure scale height is $H \approx 60$ m $\rho_{12}^{2/3} Y_n^{5/3} / g_{14}$. (In reality, the neutrons interact

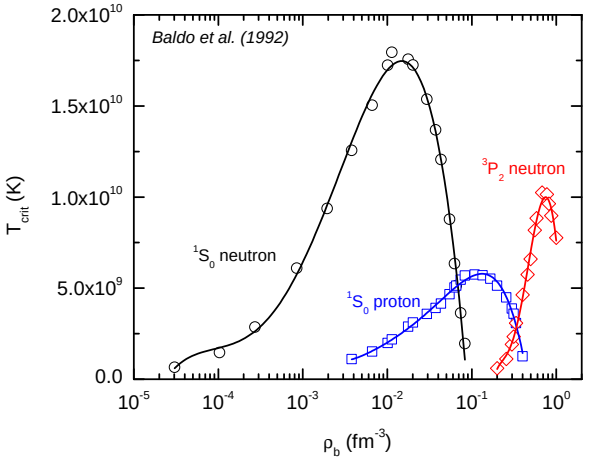

Figure 1.4: The superfluid critical temperature as a function of baryon density (from the pairing model of [3]). For $T < T_c$, the particles are superfluid. The boundary between the crust and the core is at $\rho_b \approx 0.06 - 0.09$ fm^{-3}. Taken from [7].

with each other through the strong force. This can be described by giving the neutrons an effective mass $m_n^\star$, typically about $2m_n$).

Nuclei dissolve. In the inner crust, the surrounding gas of neutrons reduces the surface energy of the nuclei compared to nuclei in vacuum. Eventually, it is no longer favorable to form nuclei; they dissolve and the neutrons and protons form homogenous nuclear matter. This transition is described in the classic paper by Baym, Bethe, and Pethick [4] and happens at a baryon density $n_b \approx 0.08\ fm^{-3}$, or $\rho \sim 10^{14}$ g cm^{-3}. The bulk nuclear matter makes up most of the star, which will have a central density $\sim 10^{15}$ g cm^{-3} depending on the mass and the core equation of state. The Fermi energies of the protons and neutrons in the core are hundreds of MeV, and exotic particles may appear at the highest densities, e.g. a pion condensate or quark matter.

Nuclear pasta. Near the base of the inner crust, the competition between the long range Coulomb repulsion between nuclei and the short range nuclear attraction can result in complex phases of matter known as pasta phases. (In condensed matter physics, this kind of system in which competing forces give rise to complex structures is known as a *frustrated* system). Whereas at low density, nuclei are spherical, in the pasta regions nuclei may take on rod-like (spaghetti) or sheet-like (lasagna) shapes. Although the pasta likely spans only about a factor of two in density, it accounts for much of the mass of the crust. An illustration of the transition through the various pasta phases is shown in Figure 1.3. It is really quite remarkable that matter at high density exhibits this complex behaviour. Matter becomes much simpler on going from the densities of terrestrial materials to white dwarf densities; complexity emerges again once the nuclear forces become important.

Pairing and superfluidity. Fermions with an attractive interaction will pair, forming

a superfluid. In neutron stars, the superfluid pairing is usually described as $^1S_0$ or $^3P_2$, a notation which describes whether the spins of the interacting nucleons is aligned or not (triplet or singlet state). One of the features of the nuclear force is that it is spin-dependent. At the low densities in the crust, the neutrons pair in the $^1S_0$ channel. The superfluid forms at temperatures below the density-dependent critical temperature $T_c(\rho)$. Calculations of $T_c(\rho)$ are highly uncertain, but typically find that T_c increases from zero at neutron drip to a maximum $T_c \sim 10^{10}$ K and then drops again at higher densities towards the base of the inner crust, possibly reaching zero again before the boundary with the core. In the core, the neutrons can again pair by in a triplet state $^3P_2$, and the protons pair in the singlet $^1S_0$. The protons are charged particles, so the proton superfluid is a superconductor.

1.2.2 Neutron star structure

Table 1.1 summarizes the different regions of the neutron star.

Table 1.1: Neutron star structure

Region	Density ρ (g cm^{-3})	Composition	State of matter	$E_{F,e}$ (MeV)	$E_{F,n}$ (MeV)	Pressure (erg cm^{-3})	Pressure scale height H (m/g_{14})
Atmosphere	≈ 1		Ideal gas Pressure ionized				
Envelope	1–$\rho_{\rm solid}$	Nuclei, e^-	Gas/Coulomb liquid, degenerate electrons	$\lesssim 1$			
Outer crust	$\rho_{\rm solid}$–$\approx 4\times10^{11}$	Nuclei, e^-	Solid lattice, degenerate electrons	$\approx 1\ (\rho_7 Y_e)^{1/3}$	—	$P_e \approx 3\times10^{24}$ $\times(\rho_7 Y_e)^{4/3}$	$30\ \rho_7^{1/3} Y_e^{4/3}$
Inner crust	4×10^{11}–10^{14}	Nuclei, n, e^-	Solid lattice, degenerate electrons, superfluid neutrons	> 27	$1.5\ \rho_{12}^{2/3} Y_n^{2/3}$	$P_n \approx 6\times10^{29}$ $\times(\rho_{12} Y_n)^{5/3}$	$60\ \rho_{12}^{2/3} Y_n^{5/3}$
Pasta	$\sim 10^{13}$–10^{14}	Non-spherical nuclei, n, e^-	Nuclear pasta degenerate electrons, superfluid neutrons				
Core	$\gtrsim 10^{14}$ ($n_b \gtrsim 0.08$ fm^{-3})	n,p,e^-,μ	Nuclear matter n,p may be superfluid	~ 100 MeV			

1.3 The Mass–Radius Relation

One of the ways to investigate neutron star interiors is to measure the radii and masses of as many different neutron stars as possible. The maximum mass of neutron stars tells us about the high density behaviour of matter. The radius of the star tells us about the matter nearer nuclear density, whether it is *stiff* or *soft* (how hard it is to compress). Here, I go through the important points that you should know about to understand the constraints from mass and radius measurements. I write equation of state as EOS.

The nucleon-nucleon interaction. The nuclear force which binds neutrons and protons into nuclei is short range, on the scale of ∼fm. The short range nature can be seen in the way that the binding energies of nuclei scale $\propto A$, whereas if all the nucleons attracted each other you would expect the binding energy to be $\propto A^2$ (for example the gravitational binding energy of an object goes as the square of the number of particles). Although attractive, the nuclear force has a repulsive core which sets a characteristic mean spacing between nucleons in nuclei. The corresponding density is known as the nuclear saturation density $n_0 \approx 0.16$ fm^{-3}.

Stiffening of the equation of state. The repulsive part of the nuclear force provides extra resistance to compression compared to a non-interacting gas. This stiffens the equation of state, giving a scaling $P \propto \rho^2$ compared to the scaling $P \propto \rho^{5/3}$ that applies for a non-interacting non-relativistic degenerate gas. The term stiffen refers to the fact that with a steeper dependence of pressure on density, a larger pressure change is needed to increase the pressure by a certain amount.

The different ways of calculating the EOS. The many-body problem of determining $P(\rho)$ for a given nuclear interaction cannot be solved exactly. A number of different methods have been applied to calculate the equation of state, a recent comprehensive review is ref. [2]. These calculations are generally calibrated to observed properties of atomic nuclei, and then extrapolated to densities above nuclear density (or sometimes the other way round – write down a theory valid at very high density and work backwards). An interesting approach is chiral effective field theory, in which a systematic perturbative expansion of the different 2-body and 3-body interactions is written down consistent with the underlying symmetries of QCD (see [11] for a review). The advantage of this approach is that it allows the theoretical uncertainties to be written down in a well-defined way, which Hebeler et al. [12] used to argue that the neutron star radius must lie in the range $\approx$ 10–14 km.

The TOV equations. Going from the equation of state $P(\rho)$ to a predicted mass–radius relation $R(M)$ requires integrating the equations of stellar structure. In general relativity, these are known as the TOV (Tolman-Oppenheimer-Volkoff) equations

$$\frac{dP}{dr} = -\frac{G}{c^2}\frac{(P+\epsilon)(m+4\pi r^3 P/c^2)}{r(r-2Gm/c^2)} \tag{1.16}$$

$$\frac{dm}{dr} = 4\pi r^2 \frac{\epsilon}{c^2} \tag{1.17}$$

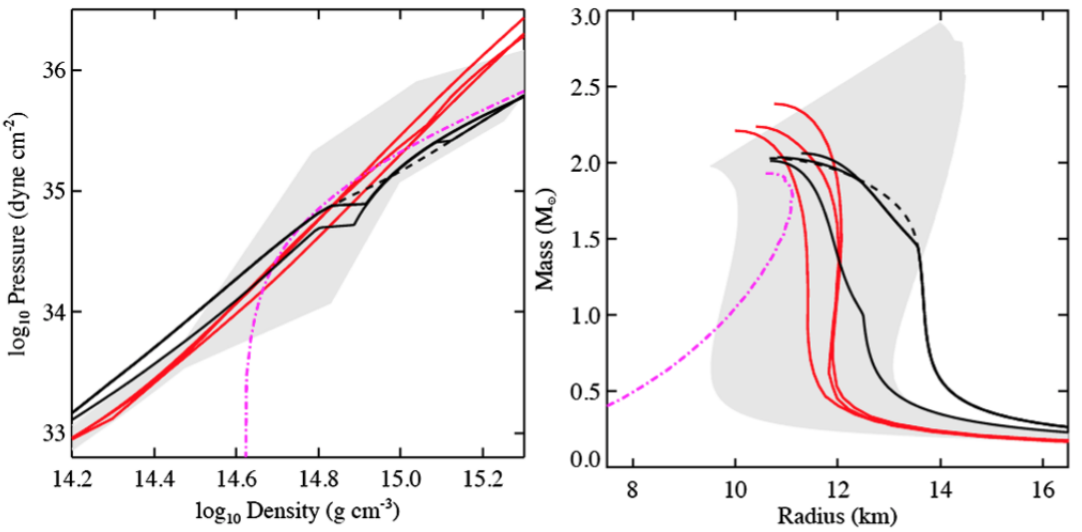

Figure 1.5: Examples of equations of state (left panel) and the resulting mass-radius relations (right panel). Taken from [23] Fig. 3 – see the caption in that article for references for the different equations of state. The grey band shows the range expected by taking the well-understood low density part of the EOS and extrapolating in different ways to high density. See also Fig. 7 of [18] which shows many more EOSs.

where $m(r)$ is the total energy contained within radius r, P is the pressure and ϵ the energy density at radius r. A useful exercise is to compare these with the usual stellar structure equations to see where the GR effects come in. You can find codes online that take $P(\rho)$ and solve the TOV equations to get $M(R)$. An example in python by Alex Deibel from MSU is at `https://github.com/adeibel/tov`.

The correspondence between the equation of state and the mass-radius relation. Figure 1.5 shows different predictions for the equation of state and corresponding mass-radius relations. An important point is that there is a mapping between $P(\rho)$ and $M(R)$ (see [16]). Low mass stars have low central densities so they depend only on the low density part of the EOS. As mass increases, the central density increases and the mass–radius relation explores the higher density part of the EOS.

Radius is roughly independent of mass. The $M(R)$ curves are very vertical in the M–R plane. This can be understood from the scaling $P_c \sim GM^2/R^4$ we used to derive the relative sizes of neutron stars and white dwarfs. For non-relativistic degeneracy pressure $P_c \propto \rho^{5/3} \propto M^{5/3}/R^5$ gives $R \propto M^{-1/3}$, the mass–radius relation for white dwarfs. Neutron stars have an equation of state closer to $P \propto \rho^2$. In that case, $P_c \propto (M/R^3)^2$, and if you follow through the argument you'll see that mass cancels and the star selects a particular radius. (A similar cancellation happens for the Chandrasekhar mass when $P \propto \rho^{4/3}$, but in that case it is radius that drops out of the equation, giving a characteristic mass). Lattimer and Prakash [15] showed that across many EOSs, $R \propto P^{1/4}$ where P is the pressure at a density about 1.5 times the saturation density, so

that a radius measurement is probing the EOS just above nuclear density.

The maximum mass. Just as there is a maximum mass for white dwarfs (the Chandrasekhar mass), neutron stars also have a maximum mass. The stiffening of the equation of state plays a crucial role in setting the maximum mass (a non-interacting Fermi gas gives a maximum mass $\lesssim 1\ M_\odot$). The extra pressure from the repulsive force raises the maximum mass. A larger maximum mass means that the equation of state at high density must be stiffer. A phase change to a different state of matter, e.g. a pion condensate, leads a softening of the EOS and a reduction in the maximum mass. The discovery of neutron stars with masses of 2 $M_\odot$ in recent years is an major constraint on equations of state. The recent review by Özel and Freire [18] is a good place to look.

Chapter 2

Neutron Star Cooling

Neutron stars are cold stars in the sense that the energies of the particles inside the star are $\gg k_B T$, so that temperature doesn't play a role in the structure of the star. But how the neutron star cools can reveal a lot about the internal composition, through both the heat capacity and the neutrino luminosity.

2.1 The Physics of Neutron Star Cooling

A recent review is [21].

Temperature evolution. The neutron star core has a very high thermal conductivity and so as the neutron star cools it stays close to isothermal. The evolution of the core temperature T is given by

$$C\frac{dT}{dt} = -L_\gamma - L_\nu, \tag{2.1}$$

where L_γ is the luminosity of the neutron star surface $L_\gamma = 4\pi R^2 \sigma T_{\rm eff}^4$ and L_ν is the neutrino luminosity of the core. Just as with white dwarf cooling, the effective temperature is related to the central temperature by constructing models of the neutron star envelope. For an iron envelope, the relation is roughly $T_{\rm eff} \approx 10^6 \text{ K } (T/10^8 \text{ K})^{1/2}$ [9], with a corresponding luminosity $L_\gamma \approx 10^{33} \text{ erg s}^{-1} \ (T/10^8 \text{ K})^2$. A light element envelope, for example helium, is less opaque and so has a larger luminosity by a factor of several for a given T. The unknown envelope composition is one of the main uncertainties in interpreting observations of cooling neutron stars.

Fast and slow neutrino emission. Neutron stars naturally cool by neutrinos through the weak reactions such as equations (1.4) and (1.5). These reactions are blocked at zero temperature because the chemical potentials are balanced (eq. 1.6). At a non-zero temperature, a small fraction of particles $\sim k_B T/E_F$ are able to undergo the weak reactions. Every time a neutron decays to a proton and then electron captures back to a neutron, neutrinos are lost because the star is optically thin to neutrinos. This process is known as the *direct URCA* process, and has an emissivity

$$\epsilon_\nu \sim 10^{26} \text{ erg cm}^{-3} \text{ s}^{-1} \left(\frac{T}{10^9 \text{ K}}\right)^6. \tag{2.2}$$

The steep temperature dependence comes from the fact that the particles involved in the reaction are degenerate (three powers of $k_B T/E_F$) and the outgoing neutrino phase space (which goes like $E_\nu^2 dE_\nu$ giving two powers of $k_B T$).

In fact, the proton fraction may be so low in the neutron star core that the direct URCA process is blocked because the reactions cannot conserve both energy and momentum. Momentum conservation requires $p_n \leq p_p + p_e$, or $n_n^{1/3} \leq n_p^{1/3} + n_e^{1/3}$. Since $n_e = n_p$, we need $n_p/n_n \geq 1/9$, which requires a high density (eq. [1.8]).

If direct URCA is suppressed, a spectator particle can act to absorb the excess momentum, e.g. $n + n \leftrightharpoons n + p + e^-$ (with neutrinos emitted in each direction), a process known as *modified URCA*. The rate is

$$\epsilon_\nu \sim 10^{20} \text{ erg cm}^{-3} \text{ s}^{-1} \left(\frac{T}{10^9 \text{ K}}\right)^8. \tag{2.3}$$

The prefactors in these expressions for ϵ_ν are uncertain by orders of magnitude, depending on the composition of the core. Handy formulas for the luminosities are $L_\nu \sim 10^{45}$ erg s^{-1} $(T/10^9 \text{ K})^6$ (direct URCA) or $L_\nu \sim 10^{39}$ erg s^{-1} $(T/10^9 \text{ K})^8$ (modified URCA). Direct URCA is an example of a "fast" neutrino process ($\propto T^6$), whereas modified URCA is a "slow" process ($\propto T^8$).

Heat capacity. The heat capacity of a degenerate Fermi gas is $c_V = \pi^2 k_B^2 T/(p_F v_F)$ per particle, where p_F and v_F are the momentum and velocity of particles at the Fermi surface (I write it this way because then this expression is valid for both non-relativistic and relativistic particles). The heat capacity of the star is given by adding up the contributions from all the particle species and integrating over the volume of the star. Since all the species are degenerate fermions, we expect the overall heat capacity to be linear in T. (This is not exactly true because the crust lattice has the Debye scaling $\propto T^3$ at low temperature, but the crust heat capacity is much smaller than the core).

Role of superfluidity. Superfluidity plays a crucial role in determining the heat capacity and the neutrino emissivity. For example, if protons are paired ($T < T_c$), then the URCA reactions are no longer allowed (there is not enough thermal energy to break pairs). The neutrino emissivity then falls to a level below the modified URCA rate set by neutron-neutron neutrino Bremsstrahlung, about a factor of ten times smaller than the modified URCA rate. The heat capacity is also affected strongly by superfluidity. If the protons or neutrons are superfluid, their heat capacity is exponentially suppressed ($\sim \exp(-T_c/T)$) and they no longer contribute. Figure 2.1 shows calculated values for heat capacity. If all particles contribute, $C \sim 10^{38}$ erg K^{-1}; if only the electrons and muons contribute, the heat capacity is an order of magnitude smaller, $C \sim 10^{37}$ erg K^{-1}.

A fascinating possibility is that the heat capacity could be even smaller if the matter in the neutron star core forms a color-flavor-locked phase (CFL phase). This is a type of quark matter in which up, down, and strange quarks are present in equal numbers and pair up to form a superfluid. Because the three types of quark (with charges $-1/3$, $-1/3$ and $+2/3$) can balance each others charge, there is no need for electrons. And because they are paired they have a suppressed heat capacity. The expected heat capacity is about 8 orders of magnitude smaller than the lepton contribution –

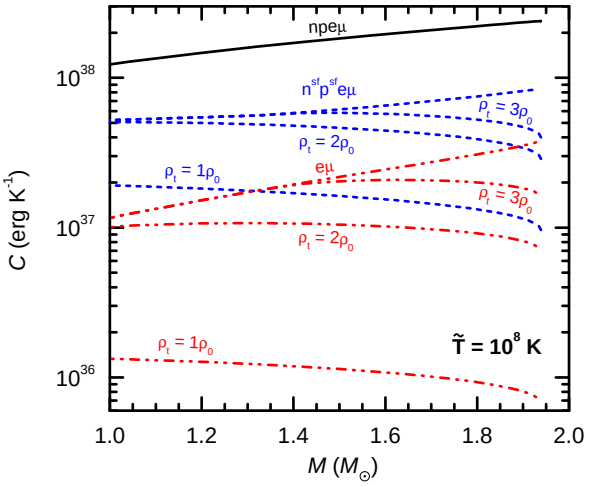

Figure 2.1: The heat capacity of the neutron star core at 10^8 K for a particular EOS. *Solid curve*: all particles contribute. *Dashed curve*: some of the neutrons and protons are superfluid, reducing the heat capacity. *Dotted*: all neutrons and protons superfluid, so only leptons contribute. *Curves labelled with* ρ_t: some of the core is in a CFL phase with vanishingly small heat capacity. Taken from [7].

so neutron stars could have very small heat capacities if this exotic phase of matter exists!

2.2 Cooling in Isolated Neutron Stars

Figure 2.2 shows predictions for the cooling curves of isolated neutron stars. Neutron stars are born hot and rapidly cool (the gravitational binding energy $GM/R \sim$ 100 MeV is equivalent to $k_B T \sim 10^{12}$ K, although neutrinos limit the temperature shortly after birth to be about 10^9 K). At first, the temperature of the neutron star surface reflects the temperature of the crust. The core has cooled quickly by neutrino emission, so is colder than the crust and the crust cools by sending heat into the core. After about 30 to 100 years, this process is complete and then the surface temperature reflects the core temperature (through the $T_{\rm eff}$–T relation). The cooling of the core is dominated by neutrino emission for about 10^6 years and afterwards by photon emission from the surface (the transition gives the change in slope of the cooling curve at about 10^6 years). The curves do a reasonable job of explaining the observed temperatures. Some neutron stars appear consistent with minimal neutrino emission; others are colder implying a larger neutrino emissivity. This could come about because more massive neutron stars reach a higher density in the core for which n_p/n_n is at a level (eq. [1.8]) where direct URCA reactions can operate.

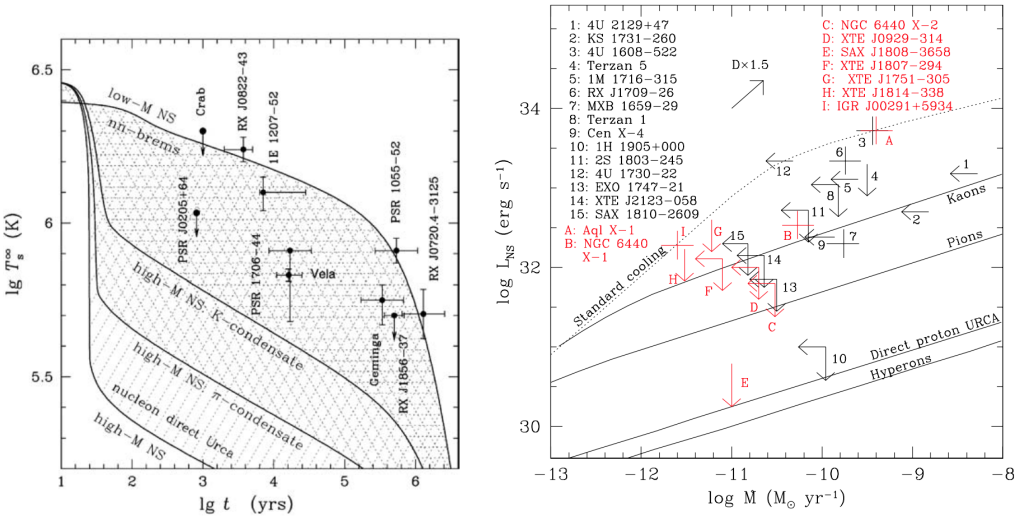

Figure 2.2: *Left:* Predictions for the cooling curves of isolated neutron stars with different core neutrino emissivity (from [24]). *Right:* The quiescent luminosity of accreting neutron stars as a function of the time-averaged accretion rate (from [13]).

2.3 Heating and Cooling in Accreting Neutron Stars

Accreting neutron stars offer a different way to study the neutrino emissivity of the core. An accreting neutron star is heated by nuclear reactions occurring in the crust as matter is compressed to higher and higher pressure [10]. The heating rate is $\approx Q_{\rm crust}\dot{M}$ where $Q_{\rm crust} \approx 1{\rm MeV}/m_u$ is the energy per unit mass released by crust reactions (m_u is the atomic mass unit). This heat flows into the core, and over time the core temperature reaches a level where the heating is balanced by neutrino losses, $L_\nu \approx Q_{\rm crust}\dot{M}$. The luminosity of a neutron star in an accreting system in quiescence (when accretion has turned off) therefore gives a measure of the neutrino emissivity. The heating rate $\langle\dot{M}\rangle Q_{\rm crust}$ tells us the neutrino luminosity from the core (assuming they balance each other on long timescales), where $\langle\dot{M}\rangle$ is the accretion rate averaged over outbursts; the measured surface temperature tells us the core temperature via the $T_{\rm eff}$–T relation. The right panel of Figure 2.2 shows observations for about 20 sources which are detected in X-rays in quiescence [13]. Some sources are consistent with modified URCA, others seem to require enhanced cooling. Again, neutron star mass may be responsible for the difference.

Accreting stars can also give information about the heat capacity, by using the accretion outbursts as a calorimeter [7]. If we know the temperature of the neutron star core before the outburst, we can measure how much the core temperature changed during the outburst as energy was added to it from the crust reactions, giving a measurement of the heat capacity $C = E/T$. In practice, accreting transients are discovered when they go into outburst; so far, we only have a lower limit on the heat capacity by assuming the core started off much colder than it ended up. This is illustrated in the left panel of Figure 2.3 which shows the temperature to which the core

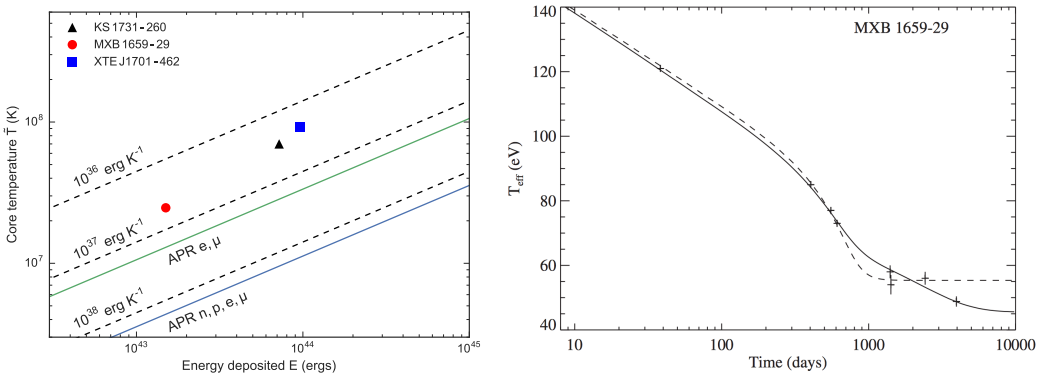

Figure 2.3: Observations of accretion neutron star transients. *Left*: Inferred core temperatures of the accreting transients MXB 1659-29, KS 1731-260, and XTE J1701-462 after outburst. The curves show the temperature to which the core would be heated by an accretion outburst for different values of core heat capacity C. Taken from [7]. *Right:* The cooling curve of MXB 1659-29 following its accretion outburst. Taken from [14].

should be heated for different values of C compared with temperature measurements for three different transients. So far, the observations rule out a heat capacity a few times smaller than the lepton value and below, e.g. a core dominated by a CFL phase is ruled out.

Accreting transients also constrain crust physics. The right panel of Figure 2.3 shows temperature measurements taken over almost a decade following the outburst of MXB 1659-29. The model is of a cooling crust that was heated up by the crust reactions and then thermally relaxed after the accretion ended, eventually coming into equilibrium with the neutron star core. The observations allow us to measure the cooling time of the crust. The cooling of the crust is described by the heat equation

$$c_P \frac{\partial T}{\partial t} = -\frac{1}{\rho}\frac{\partial F}{\partial r} = g^2 \frac{\partial}{\partial P}\left(\rho K \frac{\partial T}{\partial P}\right), \tag{2.4}$$

where we use hydrostatic balance $dP = -\rho g dr$. The cooling time is therefore

$$t_{\rm cool} \sim \frac{c_P P^2}{g^2 \rho K}, \tag{2.5}$$

so that the observations can be used to determine a combination of the heat capacity c_P, thermal conductivity K, and gravity [5].

The last observation of MXB 1659-29 (Fig. 2.3) showed evidence that the neutron star temperature dropped, in contradiction to the crust cooling model (dashed curve). The reason the model levels off is that the crust has come into thermal equilibrium with the core after about 1000 days. Including a low thermal conductivity for the pasta phase can reproduce the observed drop (solid curve) [14]. A low conductivity pasta layer had been suggested previously [20] as a way to achieve rapid magnetic

field decay and explain the lack of pulsars with spin periods greater than 10 s. The low thermal conductivity may be caused by scattering from defects that have been found in molecular dynamics simulations of pasta (Fig. 1.3).

Chapter 3

Neutron Star Magnetic Fields

3.1 The Scale of Neutron Star Magnetism

Information about neutron star magnetic fields comes from the spin down rate of pulsars, observations of cyclotron lines in accreting pulsars, and estimates based on the equilibrium spin period of accreting pulsars. The inferred dipole magnetic field strengths are $\sim 10^{11}$–3×10^{14} G for isolated neutron stars, extending down to $\lesssim 10^8$ G for some accreting neutron stars. I won't say more as you should hear more about magnetic field measurements in the afternoon.

To put these inferred magnetic field strengths in context, the mean magnetic field strength on Earth is about 1 G. This is also the mean field of the Sun, although in sunspots the local fields can exceed 1 kG. What sets the scale of neutron star magnetic fields? The largest possible internal fields are much greater than observed $\sim 10^{17}$ G (from balancing GM^2/R^4 with $B^2/8\pi$). One idea that has also been applied to white dwarfs is that the magnetic field is a *fossil field* that the neutron star inherited from its progenitor. Scaling from white dwarfs for example, and conserving magnetic flux, gives $B_{NS}/B_{WD} \sim (R_{WD}/R_{NS})^2 \sim 10^6$. The range 10^{11}–10^{15} G then becomes 10^5–10^9 G, in good agreement with the magnetic field strengths observed in magnetic white dwarfs. For white dwarfs, this idea can be tested by comparing the fraction of magnetized white dwarfs with the fraction of magnetic main sequence progenitors. For neutron stars, this is much harder because so little is known about magnetism in massive stars.

Thomson & Duncan proposed that neutron star magnetic fields are generated in a dynamo during the supernova [22]. Neutrinos leave the newly formed protoneutron star and are absorbed in the surrounding material beneath the stalled shock, generating convection. In this picture, $\gtrsim 10^{15}$ G fields can be generated by the convection[1]. The scale of the field depends on the rotation period. For fast rotation periods close to 1 ms, an α-Ω dynamo can operate giving a large scale dipole; otherwise, the field will be on smaller $\sim$ 1 km scales associated with the convective cells. In that case, a

[1]To see this, use mixing length theory to estimate the kinetic energy in the convective motions. The luminosity carried by the convection is $\sim 10^{52}$ erg s^{-1} (10^{53} ergs over seconds), giving a convective velocity $v \approx (L/4\pi r^2\rho)^{1/3} \sim 10^3$ km s^{-1} for $\rho \sim 10^{14}$ g cm^{-3} and $r \sim 10^6$ cm. The equipartition magnetic field is $B \sim (4\pi\rho v^2)^{1/2} \sim 10^{16}$ G.

superposition of many of these small dipoles could give a net global dipole of strength $\sim 10^{12}$ G, as seen in radio pulsars.

Without detailed models of the outcome of the supernova dynamo, we lack predictions for the geometry of the initial field. Differential rotation winds up poloidal field to make toroidal fields. Pure poloidal or pure toroidal configurations are unstable, suggesting that the poloidal and toroidal fields are both present and somewhere near each other in magnitude. This "twisted torus" configuration was found as a stable solution that emerged from MHD simulations of stars seeded with initially random fields. Submerged toroidal fields an order of magnitude or two above the observed dipole are possible.

3.2 The (Many) Effects of Magnetic Fields

There is a lot of interesting physics associated with neutron star magnetic fields, including:

Magnetospheres and particle acceleration. The magnetic field of a rotating star leads to creation of a magnetosphere. Goldreich & Julian showed that if you consider the neutron star to be a perfect conductor, so that the electric field vanishes in the rotating frame, there is a non-zero $\vec{E} \cdot \vec{B}$ that gives a force on charged particles orders of magnitude larger than the gravitational force. A neutron star in vacuum would quickly populate its surroundings with plasma, creating a magnetosphere. The electric field $E \sim (\Omega R/c)B$ can be cancelled by charges on closed field lines, but plasma on open fields lines flows outwards, forming a pulsar wind. The structure and electrodynamics of the pulsar magnetosphere was only solved recently, with the advent of numerical codes that can model the 3D structure of the plasma and field when the neutron star dipole and rotation axis are misaligned. Observationally, the large number of gamma-ray pulsars discovered by Fermi has led to new constraints on where particles are being accelerated in the magnetosphere.

Conductivity of the crust. A magnetic field inhibits transport of heat across field lines when the cyclotron frequency becomes large compared to the electron collision frequency ($\Omega\tau > 1$). This requires fields $B \gtrsim 10^{12}$ G in the crust. At low densities and high B such that $\hbar\omega_c > E_{F,e}$, the degenerate electrons in the crust fall into Landau levels, modifying their momentum distribution, and giving oscillations in the conductivity with depth. Observations of X-ray pulsations with large pulse amplitudes have been modelled with strong submerged toroidal magnetic fields that inhibit heat transport except very close to the magnetic pole.

Condensed surfaces. When $B \gtrsim 10^9$ G, the cyclotron energy $\hbar(eB/m_e c)$ of an electron in an atom is greater than its binding energy $\sim e^2/a_0$. The atoms become cylindrical, greatly compressed in the plane perpendicular to the magnetic field direction. These cylindrical atoms can form a condensed surface which modifies the appearance of the surface and changes the energy required to extract charged particles (e.g. in a pulsar).

Influence on the propagation of photons and the stellar spectrum. Strong magnetic

fields affect the angular distribution and frequency spectrum of emission from the neutron star surface. In fields that exceed the quantum critical field $B_Q = m_e^2 c^3/e\hbar = 4.4 \times 10^{13}$ G, where $\hbar\omega_c = m_e c^2$, QED effects become important. The vacuum becomes birefringent – different photon polarizations (relative to the magnetic field direction) travel with different speeds. This is similar to the birefringence of a plasma except that the polarizations of the two modes are different from those in a magnetized plasma. This leads to interesting physics associated with the transition from plasma to vacuum at the stellar surface, and predicted polarization signatures that could be looked for with an X-ray polarimeter. Other QED effects also can operate at high fields, such as single photon pair production, that can play a role in pulsars with strong fields.

3.3 Magnetic Field Evolution in the Crust

Magnetic activity in the form of X-ray and gamma-ray flaring and long timescale X-ray outbursts has been observed from many neutron stars, traditionally from the magnetars that were discovered that way, but also from high magnetic field radio pulsars (see [1] for a recent example). It is not obvious that neutron stars should be magnetically active - unlike the Sun for example, they do not have convective envelopes that can distort the field. The neutron star crust likely plays a key role in driving and regulating this magnetic activity.

Role of the solid crust. The crystal lattice in the crust can balance magnetic stresses, with molecular dynamics simulations indicating that the crust can support rather large strains of order $\epsilon \sim 0.1$. The shear modulus of the crust is $\mu \sim 10^{-2} P_e$ where P_e is the electron pressure. Setting $\epsilon\mu = B^2/8\pi$ gives the density below which magnetic stresses can force the crust to yield,

$$\rho_B \approx 3 \times 10^9 \text{ g cm}^{-3}\, Y_e \left(\frac{B}{10^{13}\text{ G}}\right)^{3/2} \left(\frac{\epsilon}{0.1}\right)^{-3/4}. \tag{3.1}$$

For magnetar type fields $\sim 10^{15}$ G, this extends into the inner crust. Breaking of the crust has been suggested as a gating mechanism for magnetar outbursts, that magnetic stresses build up until the crust yields. There has been a lot of work recently on how the crust yields, how energy is transferred around the star, and the role of plastic flow.

Field evolution in the crust. The magnetic field in the crust evolves according to the magnetic induction equation

$$\frac{\partial B}{\partial t} = -c\vec{\nabla} \times \vec{E} \tag{3.2}$$

where the electric field is

$$\vec{E} = \frac{\vec{J}}{\sigma} + \frac{\vec{J} \times \vec{B}}{n_e e c}. \tag{3.3}$$

The first term is the usual Ohm's law $\vec{J} = \sigma\vec{E}$; the second term is the Hall electric field. The Hall term in particular is interesting because it will cause the magnetic field

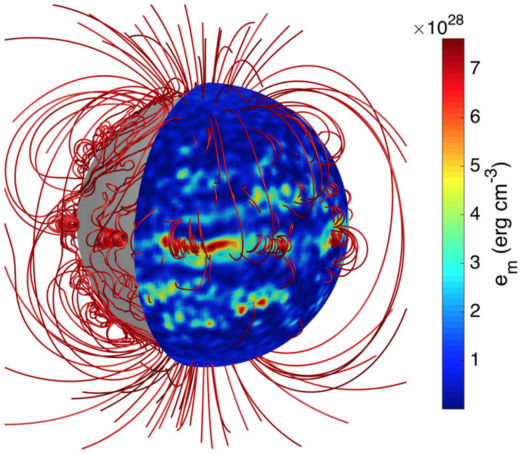

Figure 3.1: A snapshot from a 3D simulation of evolving magnetic fields in a neutron star crust. The Hall effect leads to small scale features developing near the magnetic equator with local field strengths more than an order of magnitude larger than the global dipole. Taken from [8].

configuration to spontaneously evolve. The induction equation with the Hall term can be written

$$\frac{\partial B}{\partial t} = \vec{\nabla} \times \left(\vec{v}_e \times \vec{B} \right), \tag{3.4}$$

where $\vec{v}_e = -\vec{J}/n_e e$ is the electron velocity. This looks like the "frozen field" of MHD, but now with electron velocity rather than fluid velocity. The magnetic field is advected by the electron fluid. This is a non-linear problem because the electron velocity field (the current) is itself determined by the spatial arrangement of $\vec{B}$. The timescale on which Hall effects act $t_{\rm Hall} \sim L/v_e$ is thousands of years for 10^{15} G fields deep in the crust, and so the Hall term is believed to play an important role in the magnetic activity seen in magnetars.

Bibliography

[1] R. F. Archibald, V. M. Kaspi, S. P. Tendulkar, and P. Scholz. A Magnetar-like Outburst from a High-B Radio Pulsar. *ArXiv e-prints*, August 2016.

[2] M. Baldo and G. F. Burgio. Properties of the nuclear medium. *Reports on Progress in Physics*, 75(2):026301, February 2012.

[3] M. Baldo, J. Cugnon, A. Lejeune, and U. Lombardo. Proton and neutron superfluidity in neutron star matter. *Nuclear Physics A*, 536:349–365, January 1992.

[4] G. Baym, H. A. Bethe, and C. J. Pethick. Neutron star matter. *Nuclear Physics A*, 175:225–271, November 1971.

[5] E. F. Brown and A. Cumming. Mapping Crustal Heating with the Cooling Light Curves of Quasi-Persistent Transients. ApJ, 698:1020–1032, June 2009.

[6] D. D. Clayton. *Principles of stellar evolution and nucleosynthesis*. 1983.

[7] A. Cumming, E. Brown, F. Fattoyev, C. Horowitz, D. Page, and S. Reddy. A lower limit on the heat capacity of the neutron star core. *Phys. Rev. C, submitted*, 2016.

[8] K. N. Gourgouliatos, T. S. Wood, and R. Hollerbach. Magnetic field evolution in magnetar crusts through three-dimensional simulations. *Proceedings of the National Academy of Science*, 113:3944–3949, April 2016.

[9] E. H. Gudmundsson, C. J. Pethick, and R. I. Epstein. Structure of neutron star envelopes. ApJ, 272:286–300, September 1983.

[10] P. Haensel and J. L. Zdunik. Models of crustal heating in accreting neutron stars. A&A, 480:459–464, March 2008.

[11] K. Hebeler, J. D. Holt, J. Menéndez, and A. Schwenk. Nuclear Forces and Their Impact on Neutron-Rich Nuclei and Neutron-Rich Matter. *Annual Review of Nuclear and Particle Science*, 65:150814163019008, November 2015.

[12] K. Hebeler, J. M. Lattimer, C. J. Pethick, and A. Schwenk. Constraints on Neutron Star Radii Based on Chiral Effective Field Theory Interactions. *Physical Review Letters*, 105(16):161102, October 2010.

[13] C. O. Heinke, D. Altamirano, H. N. Cohn, P. M. Lugger, S. A. Budac, M. Servillat, M. Linares, T. E. Strohmayer, C. B. Markwardt, R. Wijnands, J. H. Swank, C. Knigge, C. Bailyn, and J. E. Grindlay. Discovery of a Second Transient Low-Mass X-ray Binary in the Globular Cluster Ngc 6440. ApJ, 714:894–903, May 2010.

[14] C. J. Horowitz, D. K. Berry, C. M. Briggs, M. E. Caplan, A. Cumming, and A. S. Schneider. Disordered Nuclear Pasta, Magnetic Field Decay, and Crust Cooling in Neutron Stars. *Physical Review Letters*, 114(3):031102, January 2015.

[15] J. M. Lattimer and M. Prakash. Neutron Star Structure and the Equation of State. ApJ, 550:426–442, March 2001.

[16] L. Lindblom. Determining the nuclear equation of state from neutron-star masses and radii. ApJ, 398:569–573, October 1992.

[17] W. G. Newton. Neutron stars: A taste of pasta? *Nature Physics*, 9:396–397, July 2013.

[18] F. Ozel and P. Freire. Masses, Radii, and Equation of State of Neutron Stars. *ArXiv e-prints*, March 2016.

[19] D. Page and S. Reddy. Thermal and transport properties of the neutron star inner crust. *ArXiv e-prints*, January 2012.

[20] J. A. Pons, D. Viganò, and N. Rea. A highly resistive layer within the crust of X-ray pulsars limits their spin periods. *Nature Physics*, 9:431–434, July 2013.

[21] A. Y. Potekhin, J. A. Pons, and D. Page. Neutron Stars — Cooling and Transport. Space Sci. Rev., 191:239–291, October 2015.

[22] C. Thompson and R. C. Duncan. Neutron star dynamos and the origins of pulsar magnetism. ApJ, 408:194–217, May 1993.

[23] A. L. Watts, N. Andersson, D. Chakrabarty, M. Feroci, K. Hebeler, G. Israel, F. K. Lamb, M. C. Miller, S. Morsink, F. Özel, A. Patruno, J. Poutanen, D. Psaltis, A. Schwenk, A. W. Steiner, L. Stella, L. Tolos, and M. van der Klis. Colloquium: Measuring the neutron star equation of state using x-ray timing. *Reviews of Modern Physics*, 88(2):021001, April 2016.

[24] D. G. Yakovlev and C. J. Pethick. Neutron Star Cooling. ARA&A, 42:169–210, September 2004.